Imaging in Neurooncology

Andreas H. Jacobs,*†‡ Lutz W. Kracht,* Axel Gossmann,§ Maria A. Rüger,*† Anne V. Thomas,‡ Alexander Thiel,*‡ and Karl Herholz‡

*Max Planck-Institute for Neurological Research, †Center for Molecular Medicine (CMMC), and ‡Departments of Neurology and §Radiology at the University of Cologne, 50931 Cologne, Germany

Summary: Imaging in patients with brain tumors aims toward the determination of the localization, extend, type, and malignancy of the tumor. Imaging is being used for primary diagnosis, planning of treatment including placement of stereotaxic biopsy, resection, radiation, guided application of experimental therapeutics, and delineation of tumor from functionally important neuronal tissue. After treatment, imaging is being used to quantify the treatment response and the extent of residual tumor. At follow-up, imaging helps to determine tumor progression and to differentiate recurrent tumor growth from treatment-induced tissue changes, such as radiation necrosis. A variety of complementary imaging methods are currently being used to obtain all the information necessary to achieve the abovementioned goals. Computed tomography and magnetic resonance imaging (MRI) reveal mostly anatomical information on the tumor, whereas magnetic resonance spectroscopy and positron emission tomography (PET) give important information on the metabolic state and molecular events within the tumor. Functional MRI and functional PET, in combination with electrophysiological methods like transcranial magnetic stimulation, are being used to delineate functionally important neuronal tissue, which has to be preserved from treatment-induced damage, as well as to gather information on tumor-induced brain plasticity. In addition, optical imaging devices have been implemented in the past few years for the development of new therapeutics, especially in experimental glioma models. In summary, imaging in patients with brain tumors plays a central role in the management of the disease and in the development of improved imaging-guided therapies. **Key Words:** Gliomas, PET, MRS, FHBG, FIAU, molecular imaging.

GENERAL AND MOLECULAR ASPECTS

Primary brain tumors may arise form various cell types of the brain including glial cells, neurons, neuroglial precursor cells, pinealocytes, the meninges, choroid plexus, pericytes of the vessels, cells of the hypophysis, and lymphocytes. The incidence of primary brain tumors varies between subtypes. The most common primary brain tumors in adults are gliomas and meningiomas. For gliomas, the incidence is six to eight in 100,000, with approximately 50% belonging to malignant subtypes. Lower-grade gliomas tend to occur in younger patients, whereas higher-grade tumors are more frequent in older patients. Gliomas are divided histologically into astrocytomas, oligodendrogliomas, mixed gliomas, ependymal tumors, and tumors of the choroid plexus. Grading is performed according to the World Health Organization (WHO) criteria, taking into account the presence of nuclear changes, mitotic activity, endothelial proliferation, and necrosis.[1,2] Glioblastoma, corresponding to WHO grade IV, is the most fatal and most common primary brain neoplasm with an incidence of three to four in 100,000. Approximately 50% of all gliomas and 20% of all primary intracranial tumors are glioblastomas. Together with all intracranial neoplasms, the glioblastoma is the second most common cause of death due to an intracranial disease after stroke. Despite aggressive multimodal treatment strategies (surgery, radiation, chemotherapy) median survival of patients with gliomas is limited, depending on grade and age at diagnosis varying from 1 year for glioblastoma, to 2–3 years for grade III and to 5–10 years for a grade II glioma.

A better understanding of glial tumorgenesis is crucial for the development of specific molecular therapeutic targets to overcome current therapeutic limitations. A complex series of molecular changes occurs, which results in dysregulation of the cell cycle, alterations of

Address correspondence and reprint requests to Professor Dr. A. H. Jacobs, M.D., Laboratory for Gene Therapy and Molecular Imaging, Department of Neurology at the University of Cologne, MPI for Neurological Research, Gleuelerstrasse 50, 50931 Cologne, Germany. E-mail: Andreas.Jacobs@pet.mpin-koeln.mpg.de.

apoptosis and cell differentiation, in neovascularization as well as tumor cell migration and invasion into the brain parenchyma. Genetic alterations which play an important role in glioma development include a loss, mutation or hypermethylation of the tumor suppressor gene TP53 or other genes involved in the regulation of the cell cycle, such as cyclin-dependent kinase N2A/p16, p14ARF and primitive neuroectodermal tumor (PTEN), as well as activation or amplification of oncogenes and growth factors and/or their receptors, such as MDM2, cyclin-dependent kinase 4, cyclin D1 and D3, epidermal growth factor receptor (EGFR), vascular endothelial growth factor (VEGF), PDGFR [platelet-derived growth factor (PDGF) receptor], and transforming growth factor-β.[3–5] During progression from low-grade astrocytoma (WHO grade II) to anaplastic astrocytoma (WHO grade III) and to glioblastoma multiforme (WHO grade IV) a step-wise accumulation of genetic alterations occurs. Whereas TP53 mutation and PDGF and PDGFR-α overexpression represent early changes during low-grade glioma development, progression to anaplastic astrocytoma is associated with pRB alteration and loss of heterozygocity (LOH) of 19q, further malignant progression to glioblastoma including LOH 10q and mutations of the PTEN gene.[6] These secondary glioblastomas, which develop from better differentiated astrocytomas, can be distinguished from primary *de novo* glioblastomas on the basis of molecular genetic findings[7] with amplification and/or overexpression of the EGFR, p16 deletion, PTEN mutation, pRB alteration, and LOH 10p and 10q associated with primary glioblastoma. Most importantly, molecular alterations have been identified, which indicate therapeutic response of patients and, thus, are prognostically relevant: anaplastic oligodendrogliomas with LOH 1p and/or LOH 19q are characteristically sensitive to PCV (procarbazine, lomustine, and vincristine) chemotherapy, and patients' survival is significantly prolonged.[8–11]

An overview of the tumors in the cranial cavity is given in Table 1.[12–50]

IMAGING FOR PRIMARY DIAGNOSIS

Cranial computed tomography (CT) and magnetic resonance imaging (MRI) with and without contrast media are widely used for primary diagnosis of brain tumors. Standard T1- and T2-weighted MRIs detect brain tumors with high sensitivity. Beside primary information on the size and localization of the tumor, especially MRI provides additional information about secondary phenomena such as mass effect, edema, hemorrhage, necrosis, and signs of increased intracranial pressure at high spatial resolution and with high tissue contrast. A set of various MRI acquisitions parameters, like T1-, T2-, proton-, diffusion-, and perfusion-weighted images as well as fluid attenuated inversion recovery (FLAIR) sequences give a characteristic pattern of each tumor depending on tumor type and grade.

Most brain tumors are hypointense on T1-weighted images and hyperintense on FLAIR, T2-, and proton-weighted images. Highly proliferative active tumors such as glioblastomas lead to a destruction of the blood-brain barrier (BBB) with subsequent leakage of contrast media (FIG. 1), which is being used for diagnostic purpose in CT and T1-weighted MRI. In contrast, low-grade tumors usually have no or minimal enhancement. The contrast-enhancing lesion (T1 + Gd) corresponds histologically to a hypercellular region with neovascularization, a central hypointense area (T1) is mainly caused by tumor necrosis. Already in the CT-era, biopsies from signal changes in areas surrounding the contrast-enhancing tumor revealed the presence of migrating tumor cells. The tumor volume measured as the volume of T2 hyperintensity is the strongest predictor of overall survival in patients with supratentorial diffuse astrocytoma WHO °II and the only predictor of malignant progression.[51]

Studies on the value of diffusion-weighted imaging (DWI) MRI are ongoing. DWI is able to characterize morphological features including edema, necrosis, and viable tumor tissue by measuring differences in the apparent diffusion coefficient (ADC). DWI might be able to detect areas of tumor infiltration which are not visible on other MRIs.[52] Furthermore, DWI seems to be useful in providing a greater degree of confidence in distinguishing brain abscesses from cystic or necrotic brain tumors than conventional MRI.[53]

Moreover, dynamic contrast-enhanced MRI is a new and promising imaging tool for measuring physiological tumor properties (e.g., microvascular permeability and plasma volume; FIG. 2). The vascular hyperpermeability of tumor vessels for macromolecular solutes yields a proteinaceous exudate within the tumor interstitium that is considered a favorable milieu for the in-growth of new capillary buds. Changes in tumor vessel permeability and tumor volume as assessed by dynamic contrast enhanced perfusion MRI serve as surrogate marker for angiogenesis and allow the prediction of pathologic tumor grade[54,55] with high sensitivity but limited specificity.[56–58]

It should be pointed out that the different tissue compartments within a glioblastoma giving rise to different magnetic resonance signals have different gene and protein expression patterns.[59] Thus, there is potential for imaging-guided proteomics and microarray analysis to identify specific markers of tumor behavior.

Because intratumoral heterogeneity of brain tumors is not adequately reflected in conventional MRI because evaluation of the contrast enhancing lesion can either under- or overestimate the presence of active tumor, magnetic resonance spectroscopy (MRS) and positron

TABLE 1. *Overview of Tumors in the Cranial Cavity*

Tumor Entities (% of all primary brain tumors)	MRI/CT	PET		Ref.
		FDG*	Methionine†	
1. Gliomas				
Pilocytic astrocytoma WHO I° (<3%)	Cystic tumor with focal contrast enhancement	Variable, focally increased	Up to 2-fold	18 21
Astrocytoma WHO II° (<5%)	T1: slightly hypointense T2: hyperintense	Decreased	1- to 2-fold	See text
Anaplastic astrocytoma WHO III° (<5%)	T1: hypointense T2: hyperintense Contrast enhancement and perifocal edema	Variable	2- to 3-fold	
Glioblastoma WHO IV° (20–25%)	Irregular tumor border T1: central necrosis hypointense T2: perifocal edema hyperintense contrast enhancement	Increased	>2.5-fold	
Oligodendroglioma WHO II°/III° (<5%)	Inhomogenous tumor with focal contrast enhancement and calcifications on CCT in 70–90%	Decreased/ increased	>2.5-fold	
Oligoastrocytoma WHO II°/III° (<5%)		Decreased/ increased	2- to 3-fold	
Ependymomas (2–3%)	Characteristic localization in IVth ventricle or intramedullary; heterogenous, cystic, hemorrhages	Decreased	1.3- to 2.7-fold	40 50 36
Choroid plexus papilloma (<1%)	Characteristic localization in ventricles; sharp tumor border; gross contrast enhancement	N.A.	N.A.	
Gliomatosis cerebri	diffusely infiltrating; hyperintense (T2, FLAIR)	N.A.	N.A.	
2. Neuronal and glio neuronal tumors				
Dysembryoplastic neuroepithelial tumor (<1%)	Multicystic subcortical tumors with focal contrast enhancement	Decreased benzodiazepine receptor density as possible reason for epileptogenicity		45 27 43
Dysplastic gangliocytoma (<1%)		Increased	Increased	
Ganglioglioma (<1%)	Cortical localization, solid or cystic with calcifications and little contrast enhancement	Variable, depending on WHO grade	N.A.	26 44 34
Central neurocytoma (<1%)	Sharp tumor border, inhomogenous with cysts, necroses, calcifications, positive contrast enhancement	Increased, depending on proliferative activity	increased	35 41
3. Tumors of the pineal gland (<1%)				
Pineocytoma		N.A.	N.A.	
Pineoblastoma	Contrast enhancing	Increased	N.A.	12
Germinoma	Isointense with contrast enhancement	N.A.	N.A.	
4. Embryogenic tumors				
Medulloblastoma (20–25% <15 y.o.; 1% >20 y.o.)	Cystic tumor in 4th ventricle (75%) or cerebellum (25%); T1: hypointense; T2: hyperintense; moderate contrast enhancement	Strongly increased	Increased	24
Primitive neuroectodermal tumors (PNET)		Decreased; relatively increased in spinal localization	N.A.	24 33

(*Table continues*)

TABLE 1. *Continued*

Tumor Entities (% of all primary brain tumors)	MRI/CT	PET		Ref.
		FDG*	Methionine†	
5. Meningeal tumors				
Meningiomas (25–30%)	Localization: in 50% convexity, parasagital or falx; other localizations: sphenoid bone (15–20%), parasellar (5–10%), frontobasal (5–10%), infratentorial (10%)	Variable (0.2- to 1.8-fold)	Increased (1.3- to 3.6-fold)	14 31 17 25 38
	CT: hyperdense, calcifications (25%) MRI: T1 isointense; T2 hypointense; infiltration of bone; dural artery; dural tail sign CT/MRI: contrast enhancement and peritumoral edema	[^{68}GA]DOTATOC-PET detects somatostatin receptor expression in meningiomas		20
Hemangiopericytoma (<0.5%)		Decreased	Increased	28
6. Tumors of the region of the sella				
Craniopharyngioma (<2%)	Intrasellar (30%) and suprasellar (70%); cystic, calcifications, contrast enhancement	-[^{18}F]FDG-PET variable depending on histological type -Specific binding to D2-receptors on [^{18} F]FESP-PET differentiates adenomas of hypophysis from perisellar meningiomas and craniopharyngiomas; -Specific increase in monoaminooxidase activity on [^{11}C]Deprenyl-PET differentiates adenomas of hypophysis from perisellar meningiomas by specific increased monoaminooxidase activity		37 14 32
Adenomas of the hypophysis (5–8%)	Microadenomonas on T1 hypo- or isointense; slow contrast enhancement; macroadenomas on T1 and T2 isointense with strong contrast enhancement			
7. Tumors of cranial nerves				
Neurinoma (6–8%)	Cranial nerve VIII (90%), others: V, VII, IX–XII; sharp tumor border, T1 hypointense, T2 hyperintense, strong contrast enhancement	Iso- or hypo-metabolic	Only slight increase	15 16 39 49
8. Lymphomas				
Primary lymphoma of the CNS (2–5%)	Localization around ventricles and in basal ganglia; in 50% multiple sites; on T1 and T2 isointense, homogenous contrast enhancement, perifocal edema	Increased; FDG-PET allows differential diagnosis from toxoplasmosis	Increased	48 22 46 13
9. Metastatic tumors (≈20% of all brain tumors)				
Lung, breast, melanoma, gastrointestinal, hypernephroma	Supratentorial (90%) localized at inner border of cortex; infratentorial (10%); 50–70% multiple; 30–50% single; T1 hyperintense, T2 hypointense, ring-like contrast enhancement	Variable; screening for metastasis with [^{18}F]FDG is not recommended	N.A.	19 29 30 42 47
		[^{68}GA]DOTATOC-PET detects somatostatin receptor positive metastasis of carcinoid tumors		23

* = [^{18}F]FDG in comparison to cortical cerebral metabolic rate of glucose (CMRGlc).
† = [^{11}C]MET in comparison to contralateral control region.
N.A. = Not available.
[^{18}F]FESP = [^{18}F]fluoro-ethyl-spiperone.
[^{68}GA]DOTATOC = [^{68}GA]-1,4,7,10-tetraazacyclododecan-*N,N′,N′′,N′′′*-tetraacetacid-D-Phe-Tyr-octreoid.

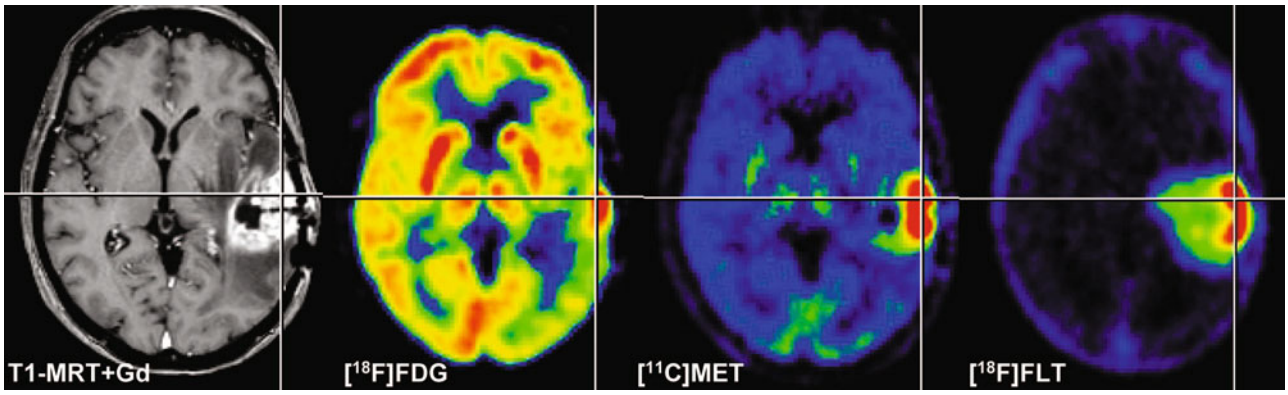

FIG. 1. Parameters of interest in the noninvasive diagnosis of brain tumors. Alteration of the blood-brain barrier and the extent of peritumoral edema are detected by MRI. Signs of increased cell proliferation can be observed by means of multi-tracer PET imaging using [^{18}F]FDG, [^{11}C]MET, and [^{18}F]FLT as specific tracers for glucose consumption, amino acid transport and DNA synthesis, respectively. Secondary phenomena, such as inactivation of ipsilateral cortical cerebral glucose metabolism, may be observed ([^{18}F]FDG) and are of prognostic relevance. Gd = gadolinium. Reproduced with permission from Jacobs AH. PET in gliomas. In: Neuroonkologie (Schlegel U, Weller M, Westphal M, eds), pp 72–76. Copyright © 2003, Thieme-Verlag. All rights reserved.[186]

emission tomography (PET) are being performed to gain additional information on metabolic and molecular tumor markers. MRS gives additional information on the real extent of the tumor and on tissue metabolites, such as N-acetylaspartate (NAA), creatine, choline, and lactate.[60] The increase of choline-containing compounds and of NAA appears to correlate best with the degree of tumor infiltration.[61,62] The appearance of creatine differentiates gliomas from metastasis, which generally lack creatine.[63] An improved automated MRS analysis approach (nosologic imaging) enables correct differentiation between low-grade glioma, high-grade glioma, meningiomas, metastasis, necrosis, and healthy tissue in up to 90% of cases and shall facilitate a noninvasive diagnosis of lesion type.[64,65] Disadvantages of MRS include its low spatial resolution, which cannot fully address the anatomical and contrast heterogeneity of brain tumors observed with MRI.

The role of PET has been primarily investigated in patients with gliomas as the most frequent and most difficult to treat primary brain tumors. PET reveals highly specific quantitative information on the metabolic state of gliomas.[66–68] PET allows the quantitative localization of expression of endogenous or exogenous genes coding for enzymes or receptors by measuring the accumulation or binding of the respective enzyme substrates or receptor binding compounds.[69–71] Depending on the radiotracer, various molecular processes can be visualized by PET, most of them relating to an increased cell proliferation within gliomas (FIG. 1). Radiolabeled 2-[^{18}F]fluoro-2-deoxy-D-glucose ([^{18}F]FDG), *methyl*-[^{11}C]-L-methionine ([^{11}C]MET) and 3′-deoxy-3′-

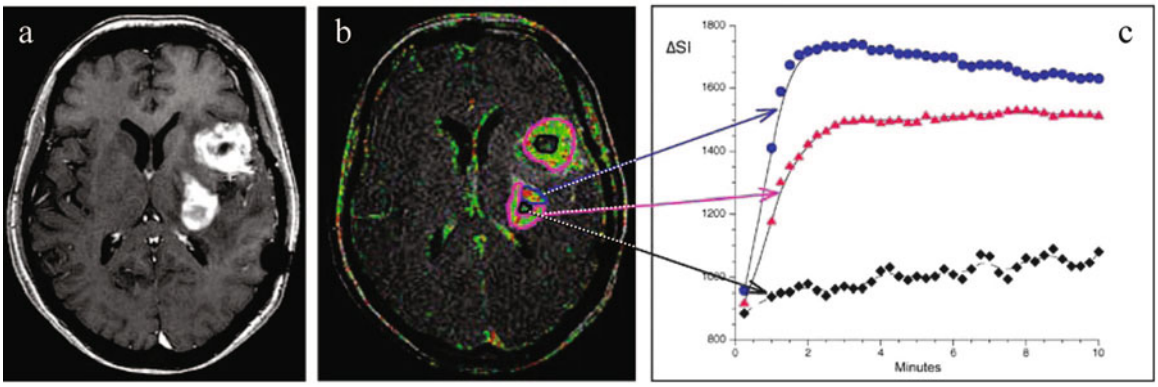

FIG. 2. Representative image of an axial T_1-weighted postcontrast sequence (a), a corresponding color coded "relative enhancement map" of a dynamic contrast enhanced three-dimensional T_1-weighted sequence (b), and signal intensity (SI) curves of different tumor areas (c) in a patient with glioblastoma multiforme. Areas with a strong uptake of contrast media show high SI values during the first 2 min with a subsequent wash out phenomena (blue region of interest and blue curve), which is indicative of a substantial microvascular leak with progressive accumulation of contrast agent in the tumor interstitial space. Areas with lower microvascular permeability values show a less pronounced tumor enhancement (pink region of interest and pink curve), whereas necrotic tumor areas only show a minor uptake of contrast media (black region of interest and black curve). Tumor heterogeneity and different areas of microvascular permeability within an individual tumor mass are characteristic findings for malignant tumors and are only visible on dynamic imaging sequences (b) and not on conventional MRIs (a).

[^{18}F]fluoro-L-thymidine ([^{18}F]FLT) are taken up by proliferating gliomas depending on their tumor grade as a reflection of increased activity of membrane transporters for glucose, ([^{18}F]FDG), amino acids ([^{11}C]MET), and nucleosides ([^{18}F]FLT) as well as increased expression of cellular hexokinase ([^{18}F]FDG) and thymidine kinase ([^{18}F]FLT) genes, which specifically phosphorylate [^{18}F]FDG and [^{18}F]FLT, respectively.

[^{18}F]FDG-PET depicts the rate of glucose uptake and has been used to detect the metabolic differences between normal brain tissue, low-grade and high-grade gliomas, and radionecrosis.[72–74] Increased intratumoral glucose consumption correlates with tumor grade, cell density, biological aggressiveness, and survival of patients in both primary and recurrent gliomas.[74–79] In general, low-grade tumors have a metabolic activity similar to white matter and higher-grade tumors, similar to gray matter (FIG. 3). A tumor-to-white matter ratio greater than 1.5 and tumor-to-gray matter ratio less than 0.6 were found to be indicative of high grade tumors with high sensitivity (94%) and limited specificity (77%).[80] Relatively benign tumors with a high FDG uptake included pilocytic astrocytoma and ganglioglioma. Pilocytic astrocytomas have a good prognosis despite exhibiting high FDG uptake and positive contrast enhancement (MRI) due to the presence of metabolically active fenestrated endothelial cells. The limited differentiation between tumor and normal gray matter by [^{18}F]FDG-PET may be improved by scanning at delayed intervals 3–7 h after tracer injection.[81] However, due to the relative high background levels of cortical glucose consumption more specific radiotracers for glioma diagnosis were developed.

The radiolabeled amino acids *methyl*-[^{11}C]-L-methionine ([^{11}C]MET), [^{11}C]-tyrosine, [^{18}F]fluoro-tyrosine and O-(2-[^{18}F]-fluoroethyl)-L-tyrosine have been shown to be more specific tracers for tumor detection and tumor delineation due to their low uptake in normal brain.[21,78,82–86] The increased methionine uptake (factor of 1.3–3.5 in comparison with a contralateral control region) is related to increased transport mediated by type L amino acid carriers.[87,88] [^{11}C]MET-uptake correlates to cell proliferation *in vitro*, the expression of Ki-67 and proliferating cell nuclear antigen, as well as to microvessel density, explaining its role as a marker for active tumor proliferation.[82,89,90] The intensity of [^{11}C]MET-uptake differentiates between WHO II° and WHO III°/IV° gliomas (FIG. 3).[21,86] Uptake is increased not only in solid parts of the tumor but also in the infiltration area.[91,92] In 80% of gliomas WHO II° [^{11}C]MET-uptake is greater than 1.5-fold of the normal brain tissue,[21] whereas glucose metabolism is reduced compared with gray matter. Most studies indicated that [^{11}C]MET-uptake is inversely correlated to prognosis,[93–95] but due to significant [^{11}C]-MET uptake also in most low-grade gliomas this relation is less close than with FDG. For WHO III°/IV° gliomas increased [^{11}C]MET-uptake is directly correlated to increased [^{18}F]FDG uptake[78,96] and exceeds the area of involvement depicted by Gd-enhanced MRI.[97] It should be pointed out that increased [^{11}C]MET uptake also depends on tumor type, with oligodendrogliomas accumulating more radiotracer than astrocytomas from the same histological grade.[21,78,98] Disadvantages of [^{11}C]methionine are its uptake in acutely ischemic and inflammatory brain tissue[99] as well as its short half-life.

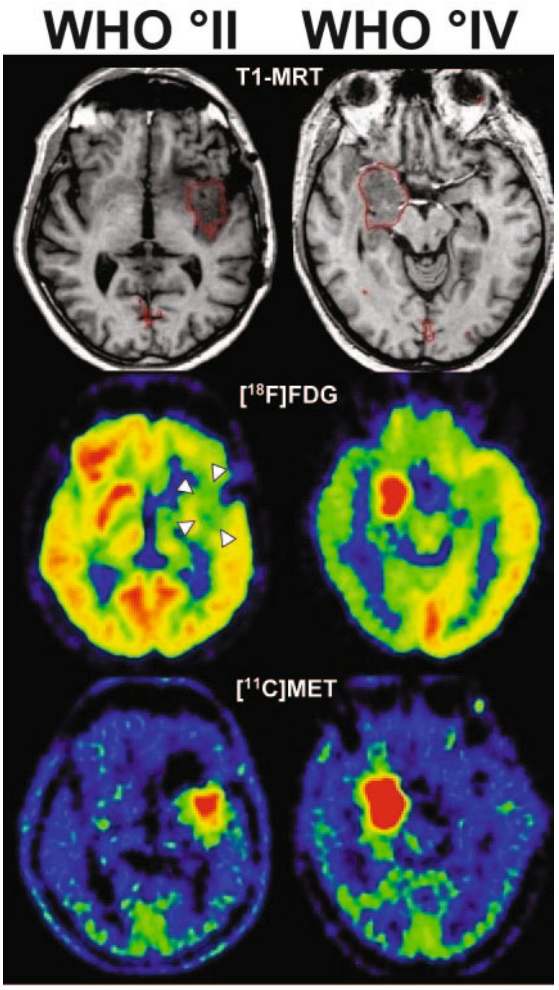

FIG. 3. Noninvasive differentiation between low- and high-grade glioma. In low-grade gliomas (WHO II°) glucose metabolism is similar to white matter (arrows) and amino acid uptake is only moderately increased. In high-grade gliomas (GBM; WHO °IV), both glucose metabolism and amino acid uptake are increased. Reproduced with permission from Jacobs AH. PET in gliomas. In: Neuroonkologie (Schlegel U, Weller M, Westphal M, eds), pp 72–76. Copyright © 2003, Thieme-Verlag. All rights reserved.[186]

The third parameter, which can be noninvasively assessed by PET is the incorporation of nucleosides into DNA in proliferating cells. Radiolabeled thymidine ([^{3}H]TdR) is the gold standard for determination of cell proliferation in cell culture, and to date ^{11}C- and ^{18}F-

labeled thymidine compounds have been radiosynthesized to allow a noninvasive assessment of tumor proliferation as well as early response to chemotherapy by PET. 3′-deoxy-3′-[^{18}F]fluoro-L-thymidine ([^{18}F]FLT) is stable *in vivo* and has been used for the evaluation of tumor proliferation primarily in extra-cranial tissues. Unpublished results in patients with gliomas indicate that [^{18}F]FLT is a promising tracer to study glioma proliferation especially in areas with high [^{18}F]FDG background. Relative [^{18}F]FLT uptake within gliomas is greater than relative [^{11}C]MET uptake (FIG. 1), indicating the possible role of [^{18}F]FLT as a more specific tumor marker than [^{18}F]FDG and [^{11}C]MET.[100–103] The overall goal is to be able to quantify chemotherapeutic effects early (within days to weeks).

A summary of MRI and PET findings in human brain tumors are given in Table 1.

IMAGING FOR PLANNING RESECTION AND RADIATION THERAPY INCLUDING DELINEATION FROM FUNCTIONAL NEURONAL TISSUE

MRI is the method of choice for tumor localization. Delineation of the tumor in three dimensions (sagittal, coronal, and axial) allows the selection of the best operative procedure. CT is being used for detection of calcifications in oligodendrogliomas, meningiomas, or craniopharyngiomas and for tumors that are located at the base of the skull. Magnetic resonance angiography is being used alone or together with conventional angiography to study the location of the tumor with respect to its vascularization. In selected patients and in specialized institutions, MRS and PET are being used in conjunction with MRI to define the real extend of the tumor.[91,104–107] Most importantly, tumors that are located in eloquent areas require preoperative functional imaging by functional MRI (fMRI) or functional PET (FIG. 4).[108–115] These combined imaging procedures are especially important in those patients where tumor growth has led to changes within the neuronal network as a result of functional brain plasticity. These changes consist either of a displacement of functional important neuronal tissue (like language areas) surrounding the lesion or in the recruitment of new brain areas that are usually not involved in the performance of a certain task.[114–116] Functional imaging studies alone can provide information about which brain areas are involved in the performance of a certain behavioral task but can not answer the diagnostically important question of whether a certain brain area is essential for that task. This additional information can be obtained by combining functional brain images with transcranial magnetic stimulation, an electrophysiological method to temporarily interfere with normal brain function[116a]. A distance of 1 cm or more between

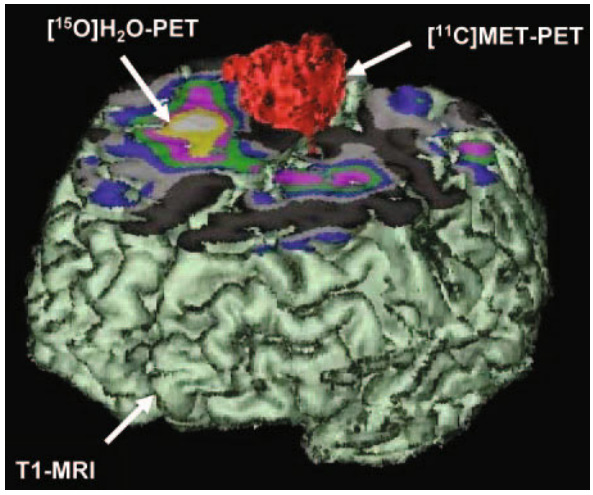

FIG. 4. Preoperative differentiation of tumor tissue from functionally important neuronal tissue through multimodal and multitracer imaging. These combined imaging procedures shall guide the neurosurgeon to operate as much tumor as possible but at the same time to leave the functionally important tissue intact. Reproduced with permission from Jacobs et al. Molecular imaging of gliomas. *Mol Imaging* 1:309–355. Copyright © 2002, MIT Press Journals. All rights reserved.[67]

the functional relevant cortex, as delineated by fMRI, and the tumor significantly reduces the risk of postoperative loss of function.[117] The evaluation of the cerebral reorganization of motor function is an essential step in predicting the risk of motor deficits in patients with an indication for operative treatment.[118] Only these combined imaging technologies will allow to maximize the spatial extent of tumor treatment and to simultaneously preserve functional relevant tissue.[119] Moreover, metabolic or molecular information derived from PET or SPECT studies is being used in some institutions for the exact planning for radio-[105] and gene therapy.[120,121] This is of special importance because tumor volume as depicted by contrast-enhanced MRI is always smaller than the tumor volume as depicted by [^{11}C]MET-PET.[97] Whether [^{11}C]MET-PET-guided extended fields of radiation have a significant influence on time to progression and overall survival has to be proven in future studies.

In recent years, diffusion tensor white matter fiber tracking and intraoperative MRI have become promising tools to guide the neurosurgeon intraoperatively. These techniques allow to maximize tumor resection without additional morbidity[122,123] by avoiding lesions to fiber tracts like the pyramidal tract.[124–126]

IMAGING FOR PLANNING STEREOTAXIC BIOPSY AND TARGETED APPLICATION OF THERAPEUTICS

Brain tumors may consist of different parts, which are heterogenous with respect to tumor grading; thus, low- and high-grade areas may be present within the same

tumor. Stereotaxic biopsy aims at the tumor sites with the highest tumor grade. Therefore, suitable targets for biopsy will have positive contrast enhancement on T1-weighted MRI, a high choline-peak on MRS, hypermetabolism on [^{18}F]FDG-PET,[127–129] and high accumulation of [^{11}C]methionine.[92,130,131] Moreover, in the development of new experimental therapies, multimodal imaging procedures help identify the most active tumor parts for targeted placement of local infusion catheters (FIG. 5). In a phase I clinical gene therapy trial, imaging the expression of endogenous genes by [^{18}F]FDG- and [^{11}C]MET-PET as direct measures for the respective gene expression and as surrogate markers for proliferation and tumor cell density was used to identify the biological active tumor portion as proper target tissue and to measure response to gene therapy (FIG. 5).[120,121]

In trials employing convection-enhanced delivery of local chemotherapeutics, DWI is being used to assess the convective process and routine diagnostic MR imaging to identify the tumor response.[132]

IMAGING FOR DETERMINATION OF TREATMENT EFFECT, TUMOR PROGRESSION, AND DIFFERENTIATION OF RECURRENT TUMOR FROM RADIATION NECROSIS

The effects of treatment should ideally be visualized with the same imaging parameters that have been used before therapy (FIG. 5). However, there are several limitations inherent in each imaging modality. On contrast-enhanced MRI, residual tumor and postsurgical changes can both result in abnormal enhancement. Therefore, MRI cannot be used postoperatively after day 3 and for several weeks because the surgical damage of the BBB, with subsequent leakage of contrast media, leads to a false-positive indicator of the presence of residual or recurrent tumor. Moreover, conventional MRI techniques usually fail to detect early effects of radio- and chemotherapy because individual treatment effects are only visible after more than 12 months,[133–135] with a substantial interobserver variability in the assessment of treatment response.[136] Especially after the application of biologically active agents (gene therapy vectors, toxins), the value of conventional MRI to detect therapy-specific changes of tumor viability is limited[137] as reviewed previously.[138]

In contrast, dynamic contrast enhanced MRI, as a surrogate marker for angiogenesis, is useful for monitoring antiangiogenic therapies in brain tumors.[139] Moreover, diffusion-weighted MRI detects therapy-induced water diffusion changes and has been suggested to provide an early surrogate marker for quantification of treatment response.[140] It was found that low values for the ADC indicating high tissue viability imply better response to radiotherapy, whereas high ADC values indicating necrosis correlate with poorer response.[141] Assessment of ADC ratios from tumor and contralateral control regions were also useful in the differentiation of radiation effects

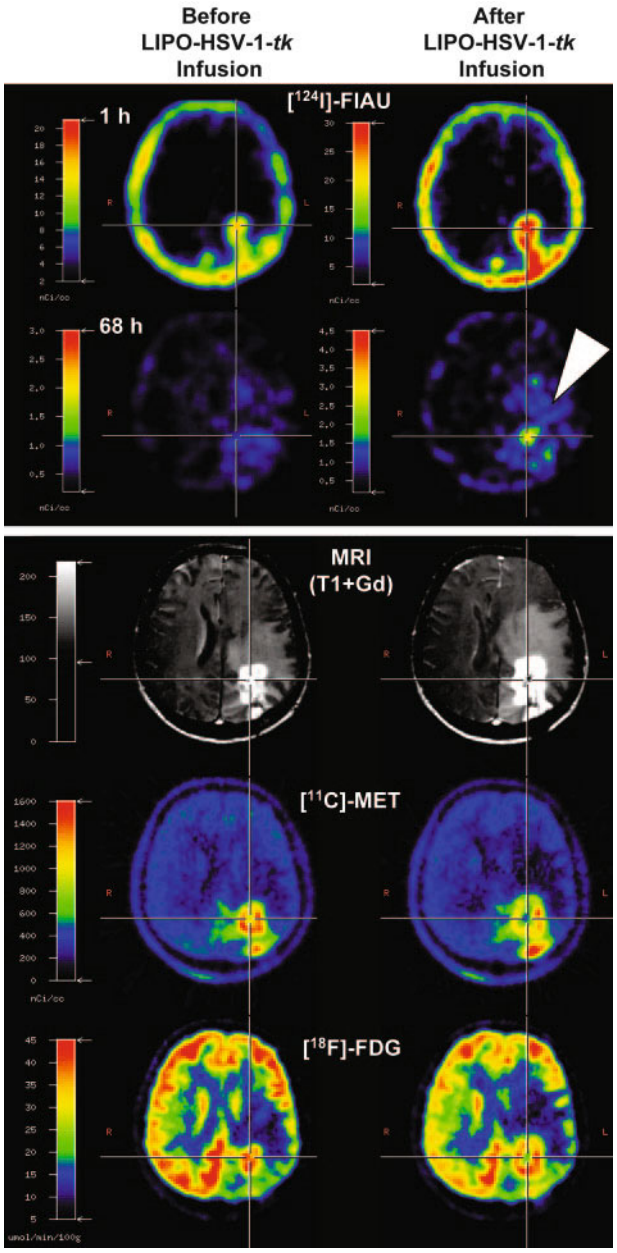

FIG. 5. Multimodal imaging for the establishment of imaging-guided experimental treatment strategies. Coregistration of [^{18}F]FIAU-, [^{11}C]MET-, [^{18}F]FDG-PET and MRI before (left column) and after (right column) targeted application (stereotactic infusion) of a gene therapy vector. The region of specific [^{124}I]-FIAU retention (68 h) within the tumor after LIPO-HSV-1-*tk* transduction (white arrow) resembles the proposed tissue dose of vector-mediated gene expression and shows signs of necrosis (cross right column; reduced methionine uptake [MET] and glucose metabolism [FDG]) after ganciclovir treatment. Reproduced with permission from Jacobs et al. Positron-emission tomography of vector-mediated gene expression in gene therapy for gliomas. *Lancet* 358:727–729. Copyright © 2001, Elsevier Limited. All rights reserved.[120]

(high ADC ratios) from tumor recurrence or progression (low ADC ratios).[142] However, it should be kept in mind that dexamethasone treatment significantly reduces the diffusivity of edematous brain,[143] thus confounding the interpretation of DWIs.

Because MRS can reliably differentiate pure tumor, pure necrosis, and normal tissue, specific changes in tumor metabolite levels as detected by MRS may be predictive for the effectiveness of experimental treatment strategies.[144] However, MRS alone may not be particularly helpful because most patients have mixed histological findings comprised of necrosis and tumor giving rise to inconclusive findings. In contrast, progression from low-grade to high-grade gliomas leads to a characteristically increased concentration of choline and a reduced NAA peak with high diagnostic accuracy.

Due to the relatively high cortical background activity, [^{18}F]FDG-PET is not suited to detect residual tumor after therapy.[145,146] Similar to structural imaging, the effects of radio- and chemotherapy can be visualized by [^{18}F]FDG-PET only after several weeks[147] with a possible transient increase of [^{18}F]FDG-uptake in the initial phase which is most likely due to infiltration of macrophages consuming [^{18}F]FDG.[148–150] At further follow-up, however, recurrent tumor and progression from low-grade to high-grade glioma can be visualized by a newly appearing hypermetabolism.[151,152] [^{18}F]FDG-PET has a sensitivity of 75% and a specificity of 81% for the detection of recurrent tumor versus radiation necrosis.[153] Moreover, in patients after stereotactic radiotherapy for brain metastasis, coregistration of [^{18}F]FDG-PET images with MRI yields an improvement of the sensitivity for the detection of recurrent tumor from 65–86%. Disadvantages of [^{18}F]FDG-PET include accumulation of [^{18}F]FDG in macrophages that may infiltrate the sites having received radiation therapy. Therefore, radiation necrosis may be indistinguishable from recurrent tumor. It should be noted that in patients receiving corticosteroids as symptomatic treatment evaluation of [^{18}F]FDG-PET may be hampered by a reduced cortex-to-white matter ratio.[154]

[^{11}C]MET-PET in contrast is much better suited to follow the effects of radiation therapy, which show as a reduction of relative methionine-uptake,[146] which may also be observed in animal models.[149] Most importantly, [^{11}C]MET-PET successfully differentiates between recurrent tumor and radiation necrosis (FIG. 6) [155] with the detection of recurrent tumor at high sensitivity and high specificity.[91,156,157] Similar results have been obtained with other tracers for amino acid transport, such as O-(2-[^{18}F]fluoroethyl)-L-tyrosine and 3-[^{123}I]iodo-α-methyl-L-tyrosine with a reliable differentiation between post-therapeutic benign lesions and tumor recurrence after treatment of low- and high-grade tumors.[158,159]

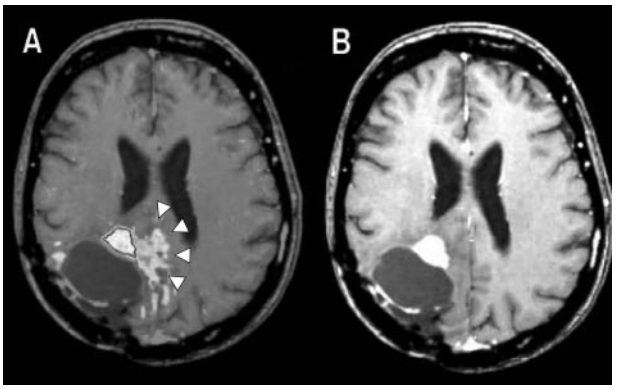

FIG. 6. Differentiation between recurrent tumor and radiation necrosis. Biopsy of this clinically worsening tumor, taken from the region with positive magnetic resonance contrast enhancement, evidenced only necrosis. However, a second biopsy from the area of increased amino acid uptake (arrowheads) revealed the findings of recurrent tumor. Reproduced with permission from Thiel et al. Enhanced accuracy in differential diagnosis of radiation necrosis by positron emission tomography-magnetic resonance imaging coregistration: technical case report. *Neurosurgery* 46:232–234. Copyright © 2000, Lippincott Williams & Wilkins. All rights reserved.[155]

IMAGING IN EXPERIMENTAL BRAIN TUMOR MODELS

Imaging studies in experimental brain tumor models over the past 10 years aimed toward 1) the development of new radiotracers for cellular proliferation and protein synthesis, 2) characterization of these tracers with respect to their ability to detect responses to radio- and chemotherapy at a relatively early stage, 3) strategies for imaging transcriptional regulation and migration of tumor cells, and 4) imaging the expression of exogenous genes carrying a marker or therapeutic function and introduced into experimental gliomas for the purpose of developing improved gene therapeutic vectors. These experimental strategies have been reviewed in detail previously.[67]

New developments aim toward 1) the detection of tumor cell migration *in vivo*,[160] 2) the establishment of *in vivo* assays for direct imaging of tumor-specific signal transduction pathways (e.g., p53-, E2F-1 and HIF-1-α regulated pathways[161–164]), 3) the design of labeled peptides binding specifically to the cell adhesion receptor integrin $\alpha(v)\beta^3$ or other tumor-specific antigens and of labeled bone marrow-derived endothelial precursor cells to allow highly specific tumor visualization and the study of glioma angiogenesis and neovascularization,[165–169] 4) the generation and *in vivo* characterization of transgenic mice with gliomas induced by signaling through Ras and Akt pathways,[170] and 5) the construction of bifunctional imaging marker and therapeutic genes to allow direct assessment of therapeutic gene expression in culture and *in vivo* models by directly corresponding assays.[171,172] Especially the design of small tumor-specific antibody fragments is an attractive way for specific detection of

tumor cells by imaging *in vivo* as well as for targeted therapy by radioimmunotherapy.

Many of the current experimental protocols investigating new drug and treatment strategies for experimental gliomas include MRI, optical or PET imaging of either the distribution of therapeutic agents,[173–175] or therapy-induced tumor-changes,[171,176–184] with the overall attempt of designing image-guided treatments.[120,121] Most intriguing for potential clinical application is the design of multifunctional nanoparticles that can be detected both by MRI and fluorescence imaging, allowing for the noninvasive preoperative assessment of the tumor and for the intraoperative visualization of tumor margins by optical imaging.[185]

SUMMARY AND CONCLUSION

Multimodal imaging (CT, MRI, PET, optical) and multitracer PET imaging 1) reveal the best set of anatomical, biochemical and molecular information on a specific tumor and, hence, a noninvasive diagnosis of lesion type and grade, 2) guide therapeutic choices, and 3) assess therapy effects. It should be pointed out that these imaging modalities are not competing with each other but give complementary information on various parameters of interest. Not every patient can be studied by these imaging technologies, and it is not necessary to do so. But these imaging technologies should be used together in selected patients to advance model systems and our understanding of the complex mechanism of glioma formation, behavior and migration and to allow the development and assessment of new therapeutic modalities including molecular targeted and gene therapies ("imaging-guided therapies").

Acknowledgments: This work is supported in part by the Ministerium für Schule, Wissenschaft und Forschung North-Rhine-Westphalia (MSWF 516-40000299), the Center for Molecular Medicine Cologne (CMMC-TV46), the Max-Planck Society, Germany and 6th Frame Work European Union grant European Molecular Imaging Laboratories (LSHC-CT-2004-503569).

REFERENCES

1. Kleihues P, Soylemezoglu F, Schauble B, Scheithauer BW, Burger PC. Histopathology, classification, and grading of gliomas. *Glia* 15:211–221, 1995.
2. Louis DN, Holland EC, Cairncross JG. Glioma classification: a molecular reappraisal. *Am J Pathol* 159:779–786, 2001.
3. Barker FG, Israel MA. Molecular genetics. In: The gliomas (Berger MS, Wilson CB, eds), pp 39–51. Philadelphia: W.B. Saunders Co., 1999.
4. Ichimura K, Bolin MB, Goike HM, Schmidt EE, Moshref A, Collins VP. Deregulation of the p14ARF/MDM2/p53 pathway is a prerequisite for human astrocytic gliomas with G1-S transition control gene abnormalities. *Cancer Res* 60:417–424, 2000.
5. Morrison RS. Growth factor mediated signaling pathways. In: The gliomas (Berger MS, Wilson CB, eds), pp 52–64. Philadelphia: W.B. Saunders Co., 1999.
6. Kleihues P, Burger PC, Collins VP, Newcomb EW, Ohgaki H, Cavenee WK. Glioblastoma. In: Pathology and genetics of tumours of the nervous system. World Health Organisation Classification of Tumours (Kleihues P, Cavenee WK, eds) pp 29–39. Lyon: IARC Press, 2000.
7. Lang FF, Miller DC, Koslow M, Newcomb EW. Pathways leading to glioblastoma multiforme: a molecular analysis of genetic alterations in 65 astrocytic tumors. *J Neurosurg* 81:427–436, 1994.
8. Cairncross JG, Ueki K, Zlatescu MC, Lisle DK, Finkelstein DM, Hammond RR et al. Specific genetic predictors of chemotherapeutic response and survival in patients with anaplastic oligodendrogliomas. *J Natl Cancer Inst* 90:1473–1479, 1998.
9. DeAngelis LM, Burger PC, Green SB, Cairncross JG. Malignant glioma: who benefits from adjuvant chemotherapy? *Ann Neurol* 44:691–695, 1998.
10. Reifenberger G, Louis DN. Oligodendroglioma: toward molecular definitions in diagnostic neuro-oncology. *J Neuropathol Exp Neurol* 62:111–126, 2003.
11. Sasaki H, Zlatescu MC, Betensky RA, Johnk LB, Cutone AN, Cairncross JG, et al. Histopathological-molecular genetic correlations in referral pathologist-diagnosed low-grade "oligodendroglioma." *J Neuropathol Exp Neurol* 61:58–63, 2002.
12. Bakheet SM, Hassounah M, Al Watban J, Homsi M, Powe J, Larsson S. F-18 FDG PET scan of a metastatic pineoblastoma. *Clin Nucl Med* 24:198–199, 1999.
13. Basso U, Brandes AA. Diagnostic advances and new trends for the treatment of primary central nervous system lymphoma. *Eur J Cancer* 38:1298–1312, 2002.
14. Bergstrom M, Muhr C, Jossan S, Lilja A, Nyberg G, Langstrom B. Differentiation of pituitary adenoma and meningioma: visualization with positron emission tomography and [11C]-L-deprenyl. *Neurosurgery* 30:855–861, 1992.
15. Borbely K, Fulham MJ, Brooks RA, Di Chiro G. PET-fluorodeoxyglucose of cranial and spinal neuromas. *J Nucl Med* 33:1931–1934, 1992.
16. Chen JM, Houle S, Ang LC, Commins D, Allan K, Nedzelski J, et al. A study of vestibular schwannomas using positron emission tomography and monoclonal antibody Ki-67. *Am J Otol* 19:840–845, 1998.
17. Cremerius U, Bares R, Weis J, Sabri O, Mull M, Schroder JM, et al. Fasting improves discrimination of grade 1 and atypical or malignant meningioma in FDG-PET. *J Nucl Med* 38:26–30, 1997.
18. Fulham MJ, Melisi JW, Nishimiya J, Dwyer AJ, Di Chiro G. Neuroimaging of juvenile pilocytic astrocytomas: an enigma. *Radiology* 189:221–225, 1993.
19. Griffeth LK, Rich KM, Dehdashti F, Simpson JR, Fusselman MJ, McGuire AH, et al. Brain metastases from non-central nervous system tumors: evaluation with PET. *Radiology* 186:37–44, 1993.
20. Henze M, Schuhmacher J, Hipp P, Kowalski J, Becker DW, Doll J, et al. PET imaging of somatostatin receptors using. *J Nucl Med* 42:1053–1056, 2001.
21. Herholz K, Holzer T, Bauer B, Schroder R, Voges J, Ernestus RI, et al. 11C-methionine PET for differential diagnosis of low-grade gliomas. *Neurology* 50:1316–1322, 1998.
22. Hoffman JM, Waskin HA, Schifter T, Hanson MW, Gray L, Rosenfeld S et al. FDG-PET in differentiating lymphoma from nonmalignant central nervous system lesions in patients with AIDS. *J Nucl Med* 34:567–575, 1993.
23. Hofmann M, Maecke H, Borner R, Weckesser E, Schoffski P, Oei L et al. Biokinetics and imaging with the somatostatin receptor PET radioligand (68)Ga-DOTATOC: preliminary data. *Eur J Nucl Med* 28:1751–1757, 2001.
24. Holthoff VA, Herholz K, Berthold F, Widemann B, Schroder R, Neubauer I, et al. In vivo metabolism of childhood posterior fossa tumors and primitive neuroectodermal tumors before and after treatment. *Cancer* 72:1394–1403, 1993.
25. Iuchi T, Iwadate Y, Namba H, Osato K, Saeki N, Yamaura A, et al. Glucose and methionine uptake and proliferative activity in meningiomas. *Neurol Res* 21:640–644, 1999.
26. Kincaid PK, El Saden SM, Park SH, Goy BW. Cerebral ganglio-

gliomas: preoperative grading using FDG-PET and 201Tl-SPECT. *AJNR Am J Neuroradiol* 19:801–806, 1998.
27. Klisch J, Juengling F, Spreer J, Koch D, Thiel T, Buchert M, et al. Lhermitte-Duclos disease: assessment with MR imaging, positron emission tomography, single-photon emission CT, and MR spectroscopy. *AJNR Am J Neuroradiol* 22:824–830, 2001.
28. Kracht LW, Bauer A, Herholz K, Terstegge K, Friese M, Schroder R, et al. Positron emission tomography in a case of intracranial hemangiopericytoma. *J Comput Assist Tomogr* 23:365–368, 1999.
29. Larcos G, Maisey MN. FDG-PET screening for cerebral metastases in patients with suspected malignancy. *Nucl Med Commun* 17:197–198, 1996.
30. Lassen U, Andersen P, Daugaard G, Holm S, Jensen M, Svarer C, et al. Metabolic and hemodynamic evaluation of brain metastases from small cell lung cancer with positron emission tomography. *Clin Cancer Res* 4:2591–2597, 1998.
31. Lippitz B, Cremerius U, Mayfrank L, Bertalanffy H, Raoofi R, Weis J et al. PET-study of intracranial meningiomas: correlation with histopathology, cellularity and proliferation rate. *Acta Neurochir Suppl* 65:108–111, 1996.
32. Lucignani G, Losa M, Moresco RM, Del Sole A, Matarrese M, Bettinardi V, et al. Differentiation of clinically non-functioning pituitary adenomas from meningiomas and craniopharyngiomas by positron emission tomography with [18F]fluoro-ethyl-spiperone. *Eur J Nucl Med* 24:1149–1155, 1997.
33. Meltzer CC, Townsend DW, Kottapally S, Jadali F. FDG imaging of spinal cord primitive neuroectodermal tumor. *J Nucl Med* 39:1207–1209, 1998.
34. Meyer PT, Spetzger U, Mueller HD, Zeggel T, Sabri O, Schreckenberger M. High F-18 FDG uptake in a low-grade supratentorial ganglioma: a positron emission tomography case report. *Clin Nucl Med* 25:694–697, 2000.
35. Mineura K, Sasajima T, Itoh Y, Sasajima H, Kowada M, Tomura N, et al. Blood flow and metabolism of central neurocytoma: a positron emission tomography study. *Cancer* 76:1224–1232, 1995.
36. Mineura K, Shioya H, Kowada M, Ogawa T, Hatazawa J, Uemura K. Subependymoma of the septum pellucidum: characterization by PET. *J Neurooncol* 32:143–147, 1997.
37. Muhr C, Bergstrom M, Lundberg PO, Hartman M, Bergstrom K, Pellettieri L et al. Malignant prolactinoma with multiple intracranial metastases studied with positron emission tomography. *Neurosurgery* 22:374–379, 1988.
38. Muhr C, Gudjonsson O, Lilja A, Hartman M, Zhang ZJ, Langstrom B. Meningioma treated with interferon-α, evaluated with [(11)C]-L-methionine positron emission tomography. *Clin Cancer Res* 7:2269–2276, 2001.
39. Nyberg G, Bergstrom M, Enblad P, Lilja A, Muhr C, Langstrom B. PET-methionine of skull base neuromas and meningiomas. *Acta Otolaryngol* 117:482–489, 1997.
40. O'Tuama LA, Phillips PC, Strauss LC, Carson BC, Uno Y, Smith QR, et al. Two-phase [11C]L-methionine PET in childhood brain tumors. *Pediatr Neurol* 6:163–170, 1990.
41. Ohtani T, Takahashi A, Honda F, Ishiuchi S, Kurihara H, Inoue T, et al. Central neurocytoma with unusually intense FDG uptake: case report. *Ann Nucl Med* 15:161–165, 2001.
42. Palm I, Hellwig D, Leutz M, Rentz K, Hellwig A, Kirsch CM, et al. [Brain metastases of lung cancer: diagnostic accuracy of positron emission tomography with fluorodeoxyglucose (FDG-PET)]. *Med Klin* 94:224–227, 1999.
43. Pirotte B, Goldman S, Baleriaux D, Brotchi J. Fluorodeoxyglucose and methionine uptake in Lhermitte-Duclos disease: case report. *Neurosurgery* 50:404–407, 2002.
44. Provenzale JM, Arata MA, Turkington TG, McLendon RE, Coleman RE. Gangliogliomas: characterization by registered positron emission tomography-MR images. *AJR Am J Roentgenol* 172:1103–1107, 1999.
45. Richardson MP, Hammers A, Brooks DJ, Duncan JS. Benzodiazepine-GABA(A) receptor binding is very low in dysembryoplastic neuroepithelial tumor: a PET study. *Epilepsia* 42:1327–1334, 2001.
46. Roelcke U, Leenders KL. Positron emission tomography in patients with primary CNS lymphomas. *J Neurooncol* 43:231–236, 1999.
47. Rohren EM, Provenzale JM, Barboriak DP, Coleman RE. Screening for cerebral metastases with FDG PET in patients undergoing whole-body staging of non-central nervous system malignancy. *Radiology* 226:181–187, 2003.
48. Rosenfeld SS, Hoffman JM, Coleman RE, Glantz MJ, Hanson MW, Schold SC. Studies of primary central nervous system lymphoma with fluorine-18-fluorodeoxyglucose positron emission tomography. *J Nucl Med* 33:532–536, 1992.
49. Sakamoto H, Nakai Y, Matsuda M, Ohashi Y, Tsuyuguchi N, Kawabe J, et al. Positron emission tomographic imaging of acoustic neuromas. *Acta Otolaryngol Suppl* 542:18–21, 2000.
50. Sasajima T, Mineura K, Itoh Y, Kowada M, Hatazawa J, Ogawa T et al. Spinal cord ependymoma: a positron emission tomographic study with (11C-methyl)-L-methionine. *Neuroradiology* 38:53–55, 1996.
51. Mariani L, Siegenthaler P, Guzman R, Friedrich D, Fathi AR, Ozdoba C, et al. The impact of tumour volume and surgery on the outcome of adults with supratentorial WHO grade II astrocytomas and oligoastrocytomas. *Acta Neurochir* 146:441–448, 2004.
52. Provenzale JM, McGraw P, Mhatre P, Guo AC, Delong D. Peritumoral brain regions in gliomas and meningiomas: investigation with isotropic diffusion-weighted MR imaging and diffusion-tensor MR imaging. *Radiology* 232:451–460, 2004.
53. Chang SC, Lai PH, Chen WL, Weng HH, Ho JT, Wang JS, et al. Diffusion-weighted MRI features of brain abscess and cystic or necrotic brain tumors: comparison with conventional MRI. *Clin Imaging* 26:227–236, 2002.
54. Preul C, Kuhn B, Lang EW, Mehdorn HM, Heller M, Link J. Differentiation of cerebral tumors using multi-section echo planar MR perfusion imaging. *Eur J Radiol* 48:244–251, 2003.
55. Roberts HC, Roberts TP, Brasch RC, Dillon WP. Quantitative measurement of microvascular permeability in human brain tumors achieved using dynamic contrast-enhanced MR imaging: correlation with histologic grade. *AJNR Am J Neuroradiol* 21: 891–899, 2000.
56. Law M, Yang S, Wang H, Babb JS, Johnson G, Cha S, et al. Glioma grading: sensitivity, specificity, and predictive values of perfusion MR imaging and proton MR spectroscopic imaging compared with conventional MR imaging. *AJNR Am J Neuroradiol* 24:1989–1998, 2003.
57. Law M, Yang S, Babb JS, Knopp EA, Golfinos JG, Zagzag D, et al. Comparison of cerebral blood volume and vascular permeability from dynamic susceptibility contrast-enhanced perfusion MR imaging with glioma grade. *AJNR Am J Neuroradiol* 25:746–755, 2004.
58. Lev MH, Ozsunar Y, Henson JW, Rasheed AA, Barest GD, Harsh GR, et al. Glial tumor grading and outcome prediction using dynamic spin-echo MR susceptibility mapping compared with conventional contrast-enhanced MR: confounding effect of elevated rCBV of oligodendrogliomas. *AJNR Am J Neuroradiol* 25:214–221, 2004.
59. Hobbs SK, Shi G, Homer R, Harsh G, Atlas SW, Bednarski MD. Magnetic resonance image-guided proteomics of human glioblastoma multiforme. *J Magn Reson Imaging* 18:530–536, 2003.
60. Meyerand ME, Pipas JM, Mamourian A, Tosteson TD, Dunn JF. Classification of biopsy-confirmed brain tumors using single-voxel MR spectroscopy. *AJNR Am J Neuroradiol* 20:117–123, 1999.
61. Croteau D, Scarpace L, Hearshen D, Gutierrez J, Fisher JL, Rock JP et al. Correlation between magnetic resonance spectroscopy imaging and image-guided biopsies: semiquantitative and qualitative histopathological analyses of patients with untreated glioma. *Neurosurgery* 49:823–829, 2001.
62. Pirzkall A, McKnight TR, Graves EE, Carol MP, Sneed PK, Wara WW et al. MR-spectroscopy guided target delineation for high-grade gliomas. *Int J Radiat Oncol Biol Phys* 50:915–928, 2001.
63. Ishimaru H, Morikawa M, Iwanaga S, Kaminogo M, Ochi M, Hayashi K. Differentiation between high-grade glioma and metastatic brain tumor using single-voxel proton MR spectroscopy. *Eur Radiol* 11:1784–1791, 2001.

64. De Edelenyi FS, Rubin C, Esteve F, Grand S, Decorps M, Lefournier V, et al. A new approach for analyzing proton magnetic resonance spectroscopic images of brain tumors: nosologic images. *Nat Med* 6:1287–1289, 2000.
65. Li X, Jin H, Lu Y, Oh J, Chang S, Nelson SJ. Identification of MRI and ^{1}H MRSI parameters that may predict survival for patients with malignant gliomas. *NMR Biomed* 17:10–20, 2004.
66. Herholz K, Wienhard K, Heiss WD. Validity of PET studies in brain tumors. *Cerebrovasc Brain Metab Rev* 2:240–265, 1990.
67. Jacobs AH, Dittmar C, Winkeler A, Garlip G, Heiss WD. Molecular imaging of gliomas. *Mol Imaging* 1:309–335, 2002.
68. Price P. PET as a potential tool for imaging molecular mechanisms of oncology in man. *Trends Mol Med* 7:442–446, 2001.
69. Heiss WD, Pawlik G, Herholz K, Wagner R, Goldner H, Wienhard K. Regional kinetic constants and cerebral metabolic rate for glucose in normal human volunteers determined by dynamic positron emission tomography of [^{18}F]-2-fluoro-2-deoxy-D-glucose. *J Cereb Blood Flow Metab* 4:212–223, 1984.
70. Phelps ME. PET: the merging of biology and imaging into molecular imaging. *J Nucl Med* 41:661–681, 2000.
71. Sokoloff L, Reivich M, Kennedy C, Des Rosiers MH, Patlak CS, Pettigrew KD, et al. The [^{14}C]deoxyglucose method for the measurement of local cerebral glucose utilization: theory, procedure, and normal values in the conscious and anesthetized albino rat. *J Neurochem* 28:897–916, 1977.
72. Heiss WD, Heindel W, Herholz K, Rudolf J, Bunke J, Jeske J, et al. Positron emission tomography of fluorine-18-deoxyglucose and image- guided phosphorus-31 magnetic resonance spectroscopy in brain tumors. *J Nucl Med* 31:302–310, 1990.
73. Herholz K, Heindel W, Luyten PR, denHollander JA, Pietrzyk U, Voges J, et al. In vivo imaging of glucose consumption and lactate concentration in human gliomas. *Ann Neurol* 31:319–327, 1992.
74. Herholz K, Pietrzyk U, Voges J, Schroder R, Halber M, Treuer H, et al. Correlation of glucose consumption and tumor cell density in astrocytomas. A stereotactic PET study. *J Neurosurg* 79:853–858, 1993.
75. Barker FG, Chang SM, Valk PE, Pounds TR, Prados MD. 18-Fluorodeoxyglucose uptake and survival of patients with suspected recurrent malignant glioma. *Cancer* 79:115–126, 1997.
76. Di Chiro G, DeLaPaz RL, Brooks RA, Sokoloff L, Kornblith PL, Smith BH et al. Glucose utilization of cerebral gliomas measured by [18F] fluorodeoxyglucose and positron emission tomography. *Neurology* 32:1323–1329, 1982.
77. Goldman S, Levivier M, Pirotte B, Brucher JM, Wikler D, Damhaut P, et al. Regional glucose metabolism and histopathology of gliomas. A study based on positron emission tomography-guided stereotactic biopsy. *Cancer* 78:1098–1106, 1996.
78. Kaschten B, Stevenaert A, Sadzot B, Deprez M, Degueldre C, Del Fiore G, et al. Preoperative evaluation of 54 gliomas by PET with fluorine-18-fluorodeoxyglucose and/or carbon-11-methionine. *J Nucl Med* 39:778–785, 1998.
79. Patronas NJ, Di Chiro G, Kufta C, Bairamian D, Kornblith PL, Simon R, et al. Prediction of survival in glioma patients by means of positron emission tomography. *J Neurosurg* 62:816–822, 1985.
80. Delbeke D, Meyerowitz C, Lapidus RL, Maciunas RJ, Jennings MT, Moots PL, et al. Optimal cutoff levels of F-18 fluorodeoxyglucose uptake in the differentiation of low-grade from high-grade brain tumors with PET. *Radiology* 195:47–52, 1995.
81. Spence AM, Muzi M, Mankoff DA, O'Sullivan SF, Link JM, Lewellen TK, et al. 18F-FDG PET of gliomas at delayed intervals: improved distinction between tumor and normal gray matter. *J Nucl Med* 45:1653–1659, 2004.
82. Chung JK, Kim YK, Kim SK, Lee YJ, Paek S, Yeo JS, et al. Usefulness of 11C-methionine PET in the evaluation of brain lesions that are hypo- or isometabolic on 18F-FDG PET. *Eur J Nucl Med Mol Imaging* 29:176–182, 2002.
83. Jager PL, Vaalburg W, Pruim J, de Vries EG, Langen KJ, Piers DA. Radiolabeled amino acids: basic aspects and clinical applications in oncology. *J Nucl Med* 42:432–445, 2001.
84. Ogawa T, Inugami A, Hatazawa J, Kanno I, Murakami M, Yasui N, et al. Clinical positron emission tomography for brain tumors: comparison of fludeoxyglucose F 18 and L-methyl-^{11}C-methionine. *AJNR Am J Neuroradiol* 17:345–353, 1996.
85. Pauleit D, Floeth F, Tellmann L, Hamacher K, Hautzel H, Muller HW, et al. Comparison of O-(2-18F-fluoroethyl)-L-tyrosine PET and 3-123I-iodo-α-methyl-L-tyrosine SPECT in brain tumors. *J Nucl Med* 45:374–381, 2004.
86. Sasaki M, Kuwabara Y, Yoshida T, Nakagawa M, Fukumura T, Mihara F, et al. A comparative study of thallium-201 SPET, carbon-11 methionine PET and fluorine-18 fluorodeoxyglucose PET for the differentiation of astrocytic tumours. *Eur J Nucl Med* 25:1261–1269, 1998.
87. Ishiwata K, Enomoto K, Sasaki T, Elsinga PH, Senda M, Okazumi S et al. A feasibility study on L-[1-carbon-11]tyrosine and L-[methyl-carbon-11]methionine to assess liver protein synthesis by PET. *J Nucl Med* 37:279–285, 1996.
88. Langen KJ, Muhlensiepen H, Holschbach M, Hautzel H, Jansen P, Coenen HH. Transport mechanisms of 3-[123I]iodo-α-methyl-L-tyrosine in a human glioma cell line: comparison with [3H]methyl]-L-methionine. *J Nucl Med* 41:1250–1255, 2000.
89. Kracht LW, Friese M, Herholz K, Schroeder R, Bauer B, Jacobs A et al. Methyl-[11C]-l-methionine uptake as measured by positron emission tomography correlates to microvessel density in patients with glioma. *Eur J Nucl Med Mol Imaging* 30:868–873, 2003.
90. Sato N, Suzuki M, Kuwata N, Kuroda K, Wada T, Beppu T et al. Evaluation of the malignancy of glioma using 11C-methionine positron emission tomography and proliferating cell nuclear antigen staining. *Neurosurg Rev* 22:210–214, 1999.
91. Kracht LW, Miletic H, Busch S, Jacobs AH, Voges J, Hoevels M, et al. Delineation of brain tumor extent with [11C]L-methionine positron emission tomography: local comparison with stereotactic histopathology. *Clin Cancer Res* 10:7163–7170, 2004.
92. Pirotte B, Goldman S, Massager N, David P, Wikler D, Vandesteene A et al. Comparison of 18F-FDG and 11C-methionine for PET-guided stereotactic brain biopsy of gliomas. *J Nucl Med* 45:1293–1298, 2004.
93. De Witte O, Goldberg I, Wikler D, Rorive S, Damhaut P, Monclus M et al. Positron emission tomography with injection of methionine as a prognostic factor in glioma. *J Neurosurg* 95:746–750, 2001.
94. Nuutinen J, Sonninen P, Lehikoinen P, Sutinen E, Valavaara R, Eronen E, et al. Radiotherapy treatment planning and long-term follow-up with [(11)C]methionine PET in patients with low-grade astrocytoma. *Int J Radiat Oncol Biol Phys* 48:43–52, 2000.
95. Ribom D, Eriksson A, Hartman M, Engler H, Nilsson A, Langstrom B et al. Positron emission tomography (11)C-methionine and survival in patients with low-grade gliomas. *Cancer* 92: 1541–1549, 2001.
96. Goldman S, Levivier M, Pirotte B, Brucher JM, Wikler D, Damhaut P, et al. Regional methionine and glucose uptake in high-grade gliomas: a comparative study on PET-guided stereotactic biopsy. *J Nucl Med* 38:1459–1462, 1997.
97. Miwa K, Shinoda J, Yano H, Okumura A, Iwama T, Nakashima T, et al. Discrepancy between lesion distributions on methionine PET and MR images in patients with glioblastoma multiforme: insight from a PET and MR fusion image study. *J Neurol Neurosurg Psychiatry* 75:1457–1462, 2004.
98. Derlon JM, Petit-Taboue MC, Chapon F, Beaudouin V, Noel MH, Creveuil C, et al. The in vivo metabolic pattern of low-grade brain gliomas: a positron emission tomographic study using 18F-fluorodeoxyglucose and 11C-L-methylmethionine. *Neurosurgery* 40:276–287, 1997.
99. Jacobs A. Amino acid uptake in ischemically compromised brain tissue. *Stroke* 26:1859–1866, 1995.
100. Krohn KA. Evaluation of alternative approaches for imaging cellular growth. *Q J Nucl Med* 45:174–178, 2001.
101. Mankoff DA, Dehdashti F, Shields AF. Characterizing tumors using metabolic imaging: PET imaging of cellular proliferation and steroid receptors. *Neoplasia* 2:71–88, 2000.
102. Mier W, Haberkorn U, Eisenhut M. [18F]FLT; portrait of a proliferation marker. *Eur J Nucl Med Mol Imaging* 29:165–169, 2002.
103. Shields AF, Grierson JR, Dohmen BM, Machulla HJ, Stayanoff

JC, Lawhorn-Crews JM, et al. Imaging proliferation in vivo with [F-18]FLT and positron emission tomography. *Nat Med* 4:1334–1336, 1998.
104. Chan AA, Lau A, Pirzkall A, Chang SM, Verhey LJ, Larson D, et al. Proton magnetic resonance spectroscopy imaging in the evaluation of patients undergoing γ knife surgery for Grade IV glioma. *J Neurosurg* 101:467–475, 2004.
105. Grosu AL, Lachner R, Wiedenmann N, Stark S, Thamm R, Kneschaurek P, et al. Validation of a method for automatic image fusion (BrainLAB System) of CT data and 11C-methionine-PET data for stereotactic radiotherapy using a LINAC: first clinical experience. *Int J Radiat Oncol Biol Phys* 56:1450–1463, 2003.
106. Pirzkall A, Li X, Oh J, Chang S, Berger MS, Larson DA, et al. 3D MRSI for resected high-grade gliomas before RT: tumor extent according to metabolic activity in relation to MRI. *Int J Radiat Oncol Biol Phys* 59:126–137, 2004.
107. Stadlbauer A, Moser E, Gruber S, Nimsky C, Fahlbusch R, Ganslandt O. Integration of biochemical images of a tumor into frameless stereotaxy achieved using a magnetic resonance imaging/magnetic resonance spectroscopy hybrid data set. *J Neurosurg* 101:287–294, 2004.
108. Fried I, Nenov VI, Ojemann SG, Woods RP. Functional MR and PET imaging of rolandic and visual cortices for neurosurgical planning. *J Neurosurg* 3:854–861, 1995.
109. Hamilton RJ, Sweeney PJ, Pelizzari CA, Yetkin FZ, Holman BL, Garada B, et al. Functional imaging in treatment planning of brain lesions. *Int J Radiat Oncol Biol Phys* 37:181–188, 1997.
110. Herholz K, Reulen HJ, von Stockhausen HM, Thiel A, Ilmberger J, Kessler J, et al. Preoperative activation and intraoperative stimulation of language- related areas in patients with glioma. *Neurosurgery* 41:1253–1260, 1997.
111. Krings T, Reinges MH, Thiex R, Gilsbach JM, Thron A. Functional and diffusion-weighted magnetic resonance images of space-occupying lesions affecting the motor system: imaging the motor cortex and pyramidal tracts. *J Neurosurg* 95:816–824, 2001.
112. Nyberg G, Andersson J, Antoni G, Lilja A, Pellettieri L, Valind S, et al. Activation PET scanning in pretreatment evaluation of patients with cerebral tumours or vascular lesions in or close to the sensorimotor cortex. *Acta Neurochir* 138:684–694, 1996.
113. Sabatini U, Pantano P, Brughitta G, Celli P, Ricci M, Lenzi G, et al. Presurgical integrated MRI/SPECT localization of the sensorimotor cortex in a patient with a low-grade astrocytoma in the rolandic area. *Neuroreport* 7:105–108, 1995.
114. Thiel A, Herholz K, von Stockhausen HM, van Leyen-Pilgram K, Pietrzyk U, Kessler J, et al. Localization of language-related cortex with 15O-labeled water PET in patients with gliomas. *Neuroimage* 7:284–295, 1998.
115. Thiel A, Herholz K, Koyuncu A, Ghaemi M, Kracht LW, Habedank B, et al. Plasticity of language networks in patients with brain tumors: a positron emission tomography activation study. *Ann Neurol* 50:620–629, 2001.
116. Nariai T, Senda M, Ishii K, Maehara T, Wakabayashi S, Toyama H, et al. Three-dimensional imaging of cortical structure, function and glioma for tumor resection. *J Nucl Med* 38:1563–1568, 1997.
116a. Thiel A, Habedank B, Winhuisen L, Herholz K, Kessler J, Haupt WF, Heiss WD. Essential language function of the right hemisphere in brain tumor patients. *Ann Neurol* 57:128–131, 2005.
117. Haberg A, Kvistad KA, Unsgard G, Haraldseth O. Preoperative blood oxygen level-dependent functional magnetic resonance imaging in patients with primary brain tumors: clinical application and outcome. *Neurosurgery* 54:902–914, 2004.
118. Baciu M, Le Bas JF, Segebarth C, Benabid AL. Presurgical fMRI evaluation of cerebral reorganization and motor deficit in patients with tumors and vascular malformations. *Eur J Radiol* 46:139–146, 2003.
119. Jannin P, Morandi X, Fleig OJ, Le Rumeur E, Toulouse P, Gibaud B, et al. Integration of sulcal and functional information for multimodal neuronavigation. *J Neurosurg* 96:713–723, 2002.
120. Jacobs A, Voges J, Reszka R, Lercher M, Gossmann A, Kracht L, et al. Positron-emission tomography of vector-mediated gene expression in gene therapy for gliomas. *Lancet* 358:727–729, 2001.
121. Voges J, Reszka R, Gossmann A, Dittmar C, Richter R, Garlip G, et al. Imaging-guided convection-enhanced delivery and gene therapy of glioblastoma. *Ann Neurol* 54:479–487, 2003.
122. Nimsky C, Fujita A, Ganslandt O, Von Keller B, Fahlbusch R. Volumetric assessment of glioma removal by intraoperative high-field magnetic resonance imaging. *Neurosurgery* 55:358–370, 2004.
123. Nimsky C, Ganslandt O, Von Keller B, Romstock J, Fahlbusch R. Intraoperative high-field-strength MR imaging: implementation and experience in 200 patients. *Radiology* 233:67–78, 2004.
124. Berman JI, Berger MS, Mukherjee P, Henry RG. Diffusion-tensor imaging-guided tracking of fibers of the pyramidal tract combined with intraoperative cortical stimulation mapping in patients with gliomas. *J Neurosurg* 101:66–72, 2004.
125. Clark CA, Barrick TR, Murphy MM, Bell BA. White matter fiber tracking in patients with space-occupying lesions of the brain: a new technique for neurosurgical planning? *Neuroimage* 20:1601–1608, 2003.
126. Henry RG, Berman JI, Nagarajan SS, Mukherjee P, Berger MS. Subcortical pathways serving cortical language sites: initial experience with diffusion tensor imaging fiber tracking combined with intraoperative language mapping. *Neuroimage* 21:616–622, 2004.
127. Hanson MW, Glantz MJ, Hoffman JM, Friedman AH, Burger PC, Schold SC et al. FDG-PET in the selection of brain lesions for biopsy. *J Comput Assist Tomogr* 15:796–801, 1991.
128. Levivier M, Goldman S, Pirotte B, Brucher JM, Baleriaux D, Luxen A et al. Diagnostic yield of stereotactic brain biopsy guided by positron emission tomography with [18F]fluorodeoxyglucose. *J Neurosurg* 82:445–452, 1995.
129. Pirotte B, Goldman S, Brucher JM, Zomosa G, Baleriaux D, Brotchi J et al. PET in stereotactic conditions increases the diagnostic yield of brain biopsy. *Stereotact Funct Neurosurg* 63:144–149, 1994.
130. Pirotte B, Goldman S, David P, Wikler D, Damhaut P, Vandesteene A, et al. Stereotactic brain biopsy guided by positron emission tomography (PET) with [F-18]fluorodeoxyglucose and [C-11]methionine. *Acta Neurochir Suppl* 68:133–138, 1997.
131. Voges J, Herholz K, Holzer T, Wurker M, Bauer B, Pietrzyk U et al. ^{11}C-methionine and ^{18}F-2-fluorodeoxyglucose positron emission tomography: a tool for diagnosis of cerebral glioma and monitoring after brachytherapy with ^{125}I seeds. *Stereotact Funct Neurosurg* 69(Pt 2):129–135, 1997.
132. Lidar Z, Mardor Y, Jonas T, Pfeffer R, Faibel M, Nass D, et al. Convection-enhanced delivery of paclitaxel for the treatment of recurrent malignant glioma: a phase I/II clinical study. *J Neurosurg* 100:472–479, 2004.
133. de Wit MC, de Bruin HG, Eijkenboom W, Sillevis Smitt PA, van den Bent MJ. Immediate post-radiotherapy changes in malignant glioma can mimic tumor progression. *Neurology* 63:535–537, 2004.
134. Hoang-Xuan K, Capelle L, Kujas M, Taillibert S, Duffau H, Lejeune J, et al. Temozolomide as initial treatment for adults with low-grade oligodendrogliomas or oligoastrocytomas and correlation with chromosome 1p deletions. *J Clin Oncol* 22:3133–3138, 2004.
135. Kumar AJ, Leeds NE, Fuller GN, Van Tassel P, Maor MH, Sawaya RE, et al. Malignant gliomas: MR imaging spectrum of radiation therapy- and chemotherapy-induced necrosis of the brain after treatment. *Radiology* 217:377–384, 2000.
136. Vos MJ, Uitdehaag BM, Barkhof F, Heimans JJ, Baayen HC, Boogerd W, et al. Interobserver variability in the radiological assessment of response to chemotherapy in glioma. *Neurology* 60:826–830, 2003.
137. Chiocca EA, Abbed KM, Tatter S, Louis DN, Hochberg FH, Barker F, et al. A phase I open-label, dose-escalation, multi-institutional trial of injection with an E1B-Attenuated adenovirus, ONYX-015, into the peritumoral region of recurrent malignant gliomas, in the adjuvant setting. *Mol Ther* 10:958–966, 2004.
138. Jacobs AH, Voges J, Kracht LW, Dittmar C, Winkeler A, Thomas A, et al. Imaging in gene therapy of patients with glioma. *J Neurooncol* 65:291–305, 2003.
139. Gossmann A, Helbich TH, Kuriyama N, Ostrowitzki S, Roberts TP, Shames DM, et al. Dynamic contrast-enhanced magnetic

resonance imaging as a surrogate marker of tumor response to anti-angiogenic therapy in a xenograft model of glioblastoma multiforme. *J Magn Reson Imaging* 15:233–240, 2002.
140. Chenevert TL, Stegman LD, Taylor JM, Robertson PL, Greenberg HS, Rehemtulla A, et al. Diffusion magnetic resonance imaging: an early surrogate marker of therapeutic efficacy in brain tumors. *J Natl Cancer Inst* 92:2029–2036, 2000.
141. Mardor Y, Roth Y, Ochershvilli A, Spiegelmann R, Tichler T, Daniels D, et al. Pretreatment prediction of brain tumors' response to radiation therapy using high b-value diffusion-weighted MRI. *Neoplasia* 6:136–142, 2004.
142. Hein PA, Eskey CJ, Dunn JF, Hug EB. Diffusion-weighted imaging in the follow-up of treated high-grade gliomas: tumor recurrence versus radiation injury. *AJNR Am J Neuroradiol* 25: 201–209, 2004.
143. Sinha S, Bastin ME, Wardlaw JM, Armitage PA, Whittle IR. Effects of dexamethasone on peritumoural oedematous brain: a DT-MRI study. *J Neurol Neurosurg Psychiatry* 75:1632–1635, 2004.
144. Ross BD, Kim B, Davidson BL. Assessment of ganciclovir toxicity to experimental intracranial gliomas following recombinant adenoviral-mediated transfer of the herpes simplex virus thymidine kinase gene by magnetic resonance imaging and proton magnetic resonance spectroscopy. *Clin Cancer Res* 1:651–657, 1995.
145. Kim EE, Chung SK, Haynie TP, Kim CG, Cho BJ, Podoloff DA, et al. Differentiation of residual or recurrent tumors from posttreatment changes with F-18 FDG PET. *Radiographics* 12:269–279, 1992.
146. Wurker M, Herholz K, Voges J, Pietrzyk U, Treuer H, Bauer B, et al. Glucose consumption and methionine uptake in low-grade gliomas after iodine-125 brachytherapy. *Eur J Nucl Med* 23:583–586, 1996.
147. Brock CS, Young H, O'Reilly SM, Matthews J, Osman S, Evans H, et al. Early evaluation of tumour metabolic response using [18F]fluorodeoxyglucose and positron emission tomography: a pilot study following the phase II chemotherapy schedule for temozolomide in recurrent high-grade gliomas. *Br J Cancer* 82: 608–615, 2000.
148. De Witte O, Hildebrand J, Luxen A, Goldman S. Acute effect of carmustine on glucose metabolism in brain and glioblastoma. *Cancer* 74:2836–2842, 1994.
149. Reinhardt MJ, Kubota K, Yamada S, Iwata R, Yaegashi H. Assessment of cancer recurrence in residual tumors after fractionated radiotherapy: a comparison of fluorodeoxyglucose, L-methionine and thymidine. *J Nucl Med* 38:280–287, 1997.
150. Yamamoto T, Nishizawa S, Maruyama I, Yoshida M, Tsuchida T, Waki A, et al. Acute effects of stereotactic radiosurgery on the kinetics of glucose metabolism in metastatic brain tumors: FDG PET study. *Ann Nucl Med* 15:103–109, 2001.
151. De Witte O, Levivier M, Violon P, Salmon I, Damhaut P, Wikler D Jr, et al. Prognostic value positron emission tomography with [18F]fluoro-2-deoxy-D-glucose in the low-grade glioma. *Neurosurgery* 39:470–476, 1996.
152. Glantz MJ, Hoffman JM, Coleman RE, Friedman AH, Hanson MW, Burger PC, et al. Identification of early recurrence of primary central nervous system tumors by [18F]fluorodeoxyglucose positron emission tomography. *Ann Neurol* 29:347–355, 1991.
153. Chao ST, Suh JH, Raja S, Lee SY, Barnett G. The sensitivity and specificity of FDG PET in distinguishing recurrent brain tumor from radionecrosis in patients treated with stereotactic radiosurgery. *Int J Cancer* 96:191–197, 2001.
154. Fulham MJ, Brunetti A, Aloj L, Raman R, Dwyer AJ, Di Chiro G. Decreased cerebral glucose metabolism in patients with brain tumors: an effect of corticosteroids. *J Neurosurg* 83:657–664, 1995.
155. Thiel A, Pietrzyk U, Sturm V, Herholz K, Hovels M, Schroder R. Enhanced accuracy in differential diagnosis of radiation necrosis by positron emission tomography-magnetic resonance imaging coregistration: technical case report. *Neurosurgery* 46:232–234, 2000.
156. Tsuyuguchi N, Takami T, Sunada I, Iwai Y, Yamanaka K, Tanaka K, et al. Methionine positron emission tomography for differentiation of recurrent brain tumor and radiation necrosis after stereotactic radiosurgery–in malignant glioma. *Ann Nucl Med* 18:291–296, 2004.
157. Van Laere K, Ceyssens S, Van Calenbergh F, De Groot T, Menten J, Flamen P, et al. Direct comparison of (18)F-FDG and (11)C-methionine PET in suspected recurrence of glioma: sensitivity, inter-observer variability and prognostic value. *Eur J Nucl Med Mol Imaging* 32:39–51, 2005.
158. Henze M, Mohammed A, Schlemmer HP, Herfarth KK, Hoffner S, Haufe S, et al. PET and SPECT for detection of tumor progression in irradiated low-grade astrocytoma: a receiver-operating-characteristic analysis. *J Nucl Med* 45:579–586, 2005.
159. Popperl G, Gotz C, Rachinger W, Gildehaus FJ, Tonn JC, Tatsch K. Value of O-(2-[(18)F]fluoroethyl)- l-tyrosine PET for the diagnosis of recurrent glioma. *Eur J Nucl Med Mol Imaging* 31: 1464–1470, 2004.
160. Su H, Forbes A, Gambhir SS, Braun J. Quantitation of cell number by a positron emission tomography reporter gene strategy. *Mol Imaging Biol* 6:139–148, 2004.
161. Doubrovin M, Ponomarev V, Beresten T, Balatoni J, Bornmann W, Finn R et al. Imaging transcriptional regulation of p53-dependent genes with positron emission tomography in vivo. *Proc Natl Acad Sci USA* 98:9300–9305, 2001.
162. Serganova I, Doubrovin M, Vider J, Ponomarev V, Soghomonyan S, Beresten T, et al. Molecular imaging of temporal dynamics and spatial heterogeneity of hypoxia-inducible factor-1 signal transduction activity in tumors in living mice. *Cancer Res* 64:6101–6108, 2004.
163. Uhrbom L, Nerio E, Holland EC. Dissecting tumor maintenance requirements using bioluminescence imaging of cell proliferation in a mouse glioma model. *Nat Med* 10:1257–1260, 2004.
164. Wen B, Burgman P, Zanzonico P, O'donoghue J, Cai S, Finn R, et al. A preclinical model for noninvasive imaging of hypoxia-induced gene expression; comparison with an exogenous marker of tumor hypoxia. *Eur J Nucl Med Mol Imaging* 31:1530–1538, 2004.
165. Anderson SA, Glod J, Arbab AS, Noel M, Ashari P, Fine HA, et al. Non-invasive MR imaging of magnetically labeled stem cells to directly identify neovasculature in a glioma model. *Blood* 105:420–425, 2004.
166. Chen X, Park R, Shahinian AH, Tohme M, Khankaldyyan V, Bozorgzadeh MH, et al. 18F-labeled RGD peptide: initial evaluation for imaging brain tumor angiogenesis. *Nucl Med Biol* 31: 179–189, 2004.
167. Haubner R, Wester HJ, Weber WA, Mang C, Ziegler SI, Goodman SL, et al. Noninvasive imaging of $\alpha(v)\beta 3$ integrin expression using 18F-labeled RGD-containing glycopeptide and positron emission tomography. *Cancer Res* 61:1781–1785, 2001.
168. Sundaresan G, Yazaki PJ, Shively JE, Finn RD, Larson SM, Raubitschek AA, et al. 124I-labeled engineered anti-CEA minibodies and diabodies allow high-contrast, antigen-specific small-animal PET imaging of xenografts in athymic mice. *J Nucl Med* 44:1962–1969, 2003.
169. van Waarde A, Buursma AR, Hospers GA, Kawamura K, Kobayashi T, Ishii K, et al. Tumor imaging with 2 σ-receptor ligands, 18F-FE-SA5845 and 11C-SA4503: a feasibility study. *J Nucl Med* 45:1939–1945, 2004.
170. Koutcher JA, Hu X, Xu S, Gade TP, Leeds N, Zhou XJ, et al. MRI of mouse models for gliomas shows similarities to humans and can be used to identify mice for preclinical trials. *Neoplasia* 4:480–485, 2002.
171. Jacobs AH, Winkeler A, Hartung M, Slack M, Dittmar C, Kummer C, et al. Improved HSV-1 amplicon vectors for proportional coexpression of PET marker and therapeutic genes. *Hum Gene Ther* 14:277–297, 2003.
172. Ponomarev V, Doubrovin M, Serganova I, Vider J, Shavrin A, Beresten T, et al. A novel triple-modality reporter gene for whole-body fluorescent, bioluminescent, and nuclear noninvasive imaging. *Eur J Nucl Med Mol Imaging* 31:740–751, 2004.
173. Hamstra DA, Lee KC, Tychewicz JM, Schepkin VD, Moffat BA, Chen M et al. The use of 19F spectroscopy and diffusion-weighted MRI to evaluate differences in gene-dependent enzyme prodrug therapies. *Mol Ther* 10:916–928, 2004.

174. Mamot C, Nguyen JB, Pourdehnad M, Hadaczek P, Saito R, Bringas JR et al. Extensive distribution of liposomes in rodent brains and brain tumors following convection-enhanced delivery. *J Neurooncol* 68:1–9, 2004.
175. Saito R, Bringas JR, McKnight TR, Wendland MF, Mamot C, Drummond DC, et al. Distribution of liposomes into brain and rat brain tumor models by convection-enhanced delivery monitored with magnetic resonance imaging. *Cancer Res* 64:2572–2579, 2004.
176. Grohn OH, Valonen PK, Lehtimaki KK, Vaisanen TH, Kettunen MI, Yla-Herttuala S, et al. Novel magnetic resonance imaging contrasts for monitoring response to gene therapy in rat glioma. *Cancer Res* 63:7571–7574, 2003.
177. Rehemtulla A, Stegman LD, Cardozo SJ, Gupta S, Hall DE, Contag CH, et al. Rapid and quantitative assessment of cancer treatment response using in vivo bioluminescence imaging. *Neoplasia* 2:491–495, 2000.
178. Ross BD, Chenevert TL, Garwood M, Kim B, Stegman LD, Ben Yoseph O, et al. Evaluation of (E)-2′-deoxy-2′-(fluoromethylene-)cytidine on the 9L rat brain tumor model using MRI. *NMR Biomed* 16:67–76, 2003.
179. Rubin JB, Kung AL, Klein RS, Chan JA, Sun Y, Schmidt K, et al. A small-molecule antagonist of CXCR4 inhibits intracranial growth of primary brain tumors. *Proc Natl Acad Sci USA* 100: 13513–13518, 2003.
180. Schmidt KF, Ziu M, Schmidt NO, Vaghasia P, Cargioli TG, Doshi S, et al. Volume reconstruction techniques improve the correlation between histological and in vivo tumor volume measurements in mouse models of human gliomas. *J Neurooncol* 68:207–215, 2004.
181. Schmidt NO, Ziu M, Carrabba G, Giussani C, Bello L, Sun Y, et al. Antiangiogenic therapy by local intracerebral microinfusion improves treatment efficiency and survival in an orthotopic human glioblastoma model. *Clin Cancer Res* 10:1255–1262, 2004.
182. Sun Y, Schmidt NO, Schmidt K, Doshi S, Rubin JB, Mulkern RV, et al. Perfusion MRI of U87 brain tumors in a mouse model. *Magn Reson Med* 51:893–899, 2004.
183. Valonen PK, Lehtimaki KK, Vaisanen TH, Kettunen MI, Grohn OH, Yla-Herttuala S, et al. Water diffusion in a rat glioma during ganciclovir-thymidine kinase gene therapy-induced programmed cell death in vivo: correlation with cell density. *J Magn Reson Imaging* 19:389–396, 2004.
184. Vooijs M, Jonkers J, Lyons S, Berns A. Noninvasive imaging of spontaneous retinoblastoma pathway-dependent tumors in mice. *Cancer Res* 62:1862–1867, 2002.
185. Kircher MF, Mahmood U, King RS, Weissleder R, Josephson L. A multimodal nanoparticle for preoperative magnetic resonance imaging and intraoperative optical brain tumor delineation. *Cancer Res* 63:8122–8125, 2003.
186. Jacobs AH. PET in gliomas. In: *Neuroonkologie* (Schlegel U, Weller M, Westphal M, eds.), pp 72−76. Thieme-Verlag, 2003.